JCTC Journal of Chemical Theory and Computation

ARTICLE

pubs.acs.org/JCTC

Assessment of TD-DFT and CC2 Methods for the Calculation of Resonance Raman Intensities: Application to *o*-Nitrophenol

Julien Guthmuller*

Institut für Physikalische Chemie, Friedrich Schiller Universität Jena, Helmholtzweg 4, 07743, Jena, Germany

ABSTRACT: The resonance Raman (RR) intensities of *o*-nitrophenol (oNP) were investigated theoretically with the aim of assessing the accuracy of excited state gradients calculated with DFT and CC2 approaches. It is found that the B3LYP and B2PLYP exchange-correlation (XC) functionals provide the best estimate of the ground state properties, while the other considered approaches present significantly less accurate vibrational frequencies and normal coordinates. Then, it is demonstrated that the use of the B3LYP force field for the ground state properties, in association with XC functionals including a large amount of HF exchange (M06-2X) or including long-range corrections (CAM-B3LYP and ωB97X) for the excited state gradient calculations, provides the most accurate RR spectra. Moreover, it is found that the RR intensities calculated with the best XC functionals show comparable accuracy to the results obtained with CC2 calculations. Finally, it is seen that the accuracy of the excited state gradients does not correlate with the accuracy of the excitation energies and oscillator strengths, for which XC functionals with a lesser amount of HF exchange (B3LYP, M06, and HSE06) provide more accurate results in the case of oNP. This indicates that the assessment of excited state gradients via the calculation of RR intensities, can provide additional information about the performance of quantum chemistry approaches in predicting excited state properties.

1. INTRODUCTION

The calculation of excited state properties for large molecules remains a challenge in quantum chemistry. Therefore, several studies have assessed the accuracy of time-dependent density functional theory (TDDFT) and of wave function based methods to calculate excitation energies of singlet and triplet excited states.[1−6] The oscillator strengths associated with transitions between singlet states were also investigated in some works.[7,8] However, much less is known about the accuracy of currently used quantum chemistry methods concerning the estimation of excited state gradients. Because excited state gradients are fundamentally important for a correct evaluation of excited state geometries and potential energy surfaces and for the subsequent treatment of excited state dynamics, a better knowledge of the performance of standard computational approaches is highly desirable.

An evaluation of the gradients can in principle be obtained from the calculated excited state geometries. However, this quantity is hard to evaluate, because experimental excited state geometries are usually not available. Nevertheless, a comparison can be made between experimental results and the calculated 0−0 excitations as well as with the simulated vibronic structure of the absorption spectrum, which can be obtained from a calculation of the Franck−Condon (FC) factors.[9−12] For example, Dierksen and Grimme[12] found that the vibronic structure of a series of large compounds is better reproduced with exchange-correlation (XC) functionals incorporating about 30−40% Hartree−Fock (HF) exchange. However, such a comparison hardly allows an estimation of the calculated geometrical displacements along the individual coordinates, due to the usually limited resolution of the vibronic structure in the experimental spectra. On the other hand, resonance Raman (RR) spectroscopy[13−15] provides the possibility to assess the excited state gradients separately, i.e., along each vibrational coordinate. Indeed, within the so-called short-time approximation[16] (STA), the RR intensities are directly related to the excited state gradients evaluated at the FC point. In this respect, the calculation of RR intensities and their comparison with experimental data offers an opportunity to gain more knowledge about the ability of standard quantum chemistry methods to determine excited state gradients.

This study initiates such an investigation by considering the prototype molecule of *o*-nitrophenol (oNP) (Figure 1). The RR spectrum of this compound was already investigated experimentally by Wang et al.[17] in a cyclohexane solution, and it was shown to present a rich pattern of 15 RR active vibrations. The RR measurements were performed in resonance with the first absorption band, which is associated with the first singlet excited state. First, this experimental band displays a large broadening with no resolved vibronic structure. Second, the measured RR spectra at excitation wavelengths of 355 and 369 nm show small differences in their relative RR intensities. These facts indicate that the use of the STA for the evaluation of the relative RR intensities is adequate in this case. Thus, the purpose of this contribution is to assess the accuracy of several XC functionals within the framework of TDDFT calculations as well as of the second-order approximate coupled cluster singles and doubles[18] (CC2) methods. These computational approaches are widely applied for determining excited state properties, mostly due to their good compromise between accuracy and computational cost. Therefore, an initial investigation of their performance is useful before a larger set of systems is considered.

The paper is organized as follows. Section 2 describes the employed approximations and computational methods. Section

Received: January 5, 2011
Published: March 24, 2011

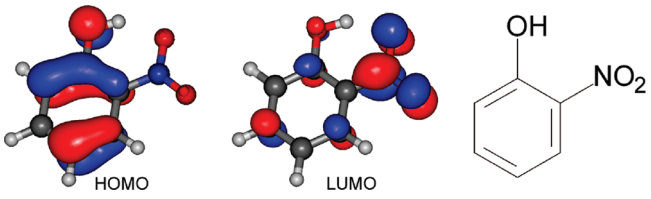

Figure 1. Structure of *o*-nitrophenol and molecular orbitals involved in the dominant excited state (B3LYP).

3.1 provides the assignment of the oNP vibrational frequencies, which is required before the RR spectra can be assessed. The vertical excitation energies and oscillator strengths are presented in section 3.2. Then, the accuracy of the considered theoretical methods for the evaluation of RR intensities is discussed in section 3.3, and conclusions are given in section 4.

2. COMPUTATIONAL METHODS

The geometry, harmonic vibrational frequencies, and normal coordinates of the ground state were obtained with the Gaussian 09 program[19] by means of density functional theory (DFT) and second-order Møller−Plesset[20] (MP2) calculations. The DFT calculations were performed with the BLYP,[21,22] B3LYP,[23,22] HSE06[24] (HSEh1PBE), CAM-B3LYP,[25] M06-2X,[26] ωB97X,[27] and B2PLYP[28] XC functionals in association with the 6-311++G(2df,p) basis set. To correct for the lack of anharmonicity and the approximate treatment of electron correlation,[29] the harmonic frequencies obtained with the B3LYP, B2PLYP, HSE06, MP2, CAM-B3LYP, M06-2X, and ωB97X force fields were scaled by factors of 0.98, 0.98, 0.96, 0.96, 0.95, 0.95, and 0.95, respectively. Additionally, the effects of the solvent cyclohexane (ε = 2.0165) on the ground state properties were taken into account by the integral equation formalism of the polarizable continuum model[30] (IEFPCM).

The vertical excitation energies, oscillator strengths, and analytical Cartesian energy derivatives of the excited states (gradients) were obtained from TDDFT calculations employing the 6-311++G(2df,p) basis set. The TDDFT calculations were performed by using the same XC functionals as for the ground state properties. Moreover, the excited state properties were also determined with all previously mentioned XC functionals in addition to M06,[26] B3LYP-35,[31] BMK,[32] and ωB97[27] by employing the B3LYP and B2PLYP ground state geometries, frequencies, and normal coordinates. The effects of the solvent were approximated with the IEFPCM model, and the nonequilibrium procedure of solvation was used for the computation of the excitation energies and excited state gradients.

The excitation energies, oscillator strengths, and gradients of the excited states were also evaluated with the second-order approximate coupled cluster singles and doubles[18] (CC2) and spin-component scaled CC2[5] (SCS-CC2) approaches. These calculations were performed with the RICC2 module[33,34] of the TURBOMOLE 6.2 program,[35] thus making use of the resolution of the identity approximation. The def2-QZVPP basis set[36] and its associated auxiliary basis set were employed for all (SCS)-CC2 calculations. Moreover, SCS-CC2 computations made use of scale parameters[5] for the opposite-spin and same-spin components equal to c_{os} = 6/5 and c_{ss} = 1/3, respectively. All (SCS)-CC2 calculations were performed in a vacuum using the B3LYP, B2PLYP, and MP2 ground state geometries obtained with the Gaussian 09 program.

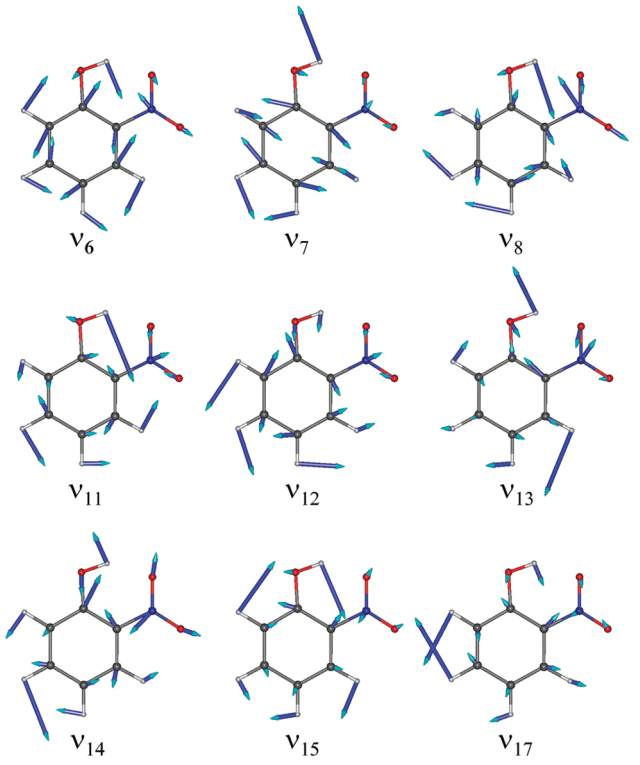

Figure 2. Nuclear displacements of several vibrational normal modes of *o*-nitrophenol calculated at the B3LYP/6-311++G(2df,p) level of approximation.

The relative RR intensities were obtained within the short-time approximation.[16] In the STA, the RR intensity for a fundamental transition $0 \rightarrow 1_l$ can be obtained from the partial derivatives of the excited state electronic energy (E^e) along the lth normal coordinate (Q_l) evaluated at the ground state equilibrium geometry:

$$I_{0 \rightarrow 1_l} \propto \frac{1}{\omega_l}\left(\frac{\partial E^e}{\partial Q_l}\right)_0^2 \quad (1)$$

where ω_l is the frequency of the lth normal mode. These gradients were obtained from the analytical derivatives of the excited state electronic energy (E^e) along the nonmass-weighted Cartesian coordinates according to the relation

$$\left(\frac{\partial E^e}{\partial Q}\right)_0 = L^T M^{-1/2}\left(\frac{\partial E^e}{\partial x}\right)_0 \quad (2)$$

where M is the matrix containing the atomic masses, L is the orthogonal matrix obtained from the solution of the ground state normal mode eigenvalue problem and connects the mass-weighted Cartesian coordinates to the mass-weighted normal coordinates, and $(\partial E^e/\partial Q)_0$ and $(\partial E^e/\partial x)_0$ are column vectors containing the derivatives along the normal coordinates and Cartesian coordinates, respectively.

Finally, the relative nonresonant Raman intensities at the standard excitation wavelength of 1064 nm were obtained according to the relation

$$I_{0 \rightarrow 1_l} \propto \omega_L(\omega_L - \omega_l)^3(45a_l^2 + 7\gamma_l^2) \quad (3)$$

where a_l^2 and γ_l^2 are invariants for randomly oriented molecules[37,15] evaluated from the analytical derivatives of the

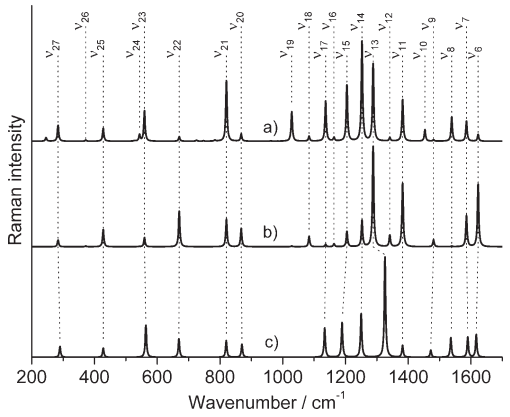

Figure 3. Assignment of the vibrational frequencies. (a) B3LYP/6-311++G(2df,p) Raman spectrum in cyclohexane at 1064 nm. (b) B3LYP/6-311++G(2df,p) RR spectrum in cyclohexane calculated within the STA. (c) Experimental RR spectrum in cyclohexane at 355 nm; the spectrum is reconstructed from the cross-sections reported in Table 4 of ref 17. All of the spectra are normalized with respect to the most intense band, and a Lorentzian function with a fwhm of 5 cm^{-1} is employed to broaden the transitions.

polarizability tensor along the normal coordinates $(\partial\alpha_{ij}/\partial Q_I)_0$. These derivatives were obtained from the B3LYP ground state vibrational frequency calculation performed with Gaussian 09.

3. RESULTS AND DISCUSSION

3.1. Assignment of the *o*-Nitrophenol Vibrational Frequencies. To assess the accuracy of the calculated RR intensities and therefore the excited state gradients, it is first necessary to assign unambiguously the experimental frequencies to the theoretical vibrational modes (Figure 2). Assignments of the oNP vibrations were already reported in the literature[38,17] and were deduced by comparing theoretical (DFT/B3LYP) frequencies and IR intensities with experimental frequencies obtained from IR, Raman, and RR spectra. Therefore, the assignment of the fundamental transitions in the 200−1700 cm^{-1} wavenumber range is first re-examined. This is performed by simulating the Raman and RR intensities and by comparing them to the previously reported experimental spectra. To this aim, Figure 3 shows the calculated Raman and RR spectra obtained with the B3LYP XC functional as well as the experimental RR spectrum, which was reconstructed from the RR cross-sections reported in Table 4 of ref 17. It should be mentioned that the same mode numbering as the one employed by Kovács et al.[38] and Wang et al.[17] is used for the fundamental vibrations with an in-plane symmetry. Additionally, the calculated vibrational frequencies are reported in Table 1 and are compared to experimental RR frequencies recorded in cyclohexane solution and to Raman frequencies recorded in CCl_4 solution.

The assignment deduced by comparing the theoretical (B3LYP) and experimental Raman spectra is found in excellent agreement with the one reported by Kovács et al.[38] The only exception concerns the experimental Raman active vibration at 668 cm^{-1}, which is here assigned to the ν_{22} mode at 670 cm^{-1} (B3LYP) instead of a vibration of out-of-plane symmetry. It can also be mentioned that the ν_9, ν_{12}, and ν_{26} vibrations were not assigned, because they are not visible in the experimental Raman spectrum. This fact is in agreement with their weak calculated Raman intensity (Figure 3). However, these three vibrations (ν_9, ν_{12}, ν_{26}) with frequencies of 1480.8, 1341.3, and 372.2 cm^{-1}, respectively, can be assigned to the experimental IR bands in CCl_4 solution[38] at 1479, 1333, and 372 cm^{-1}, respectively.

Table 1. Experimental and Calculated Vibrational Frequencies

	calculated frequencies[a] (cm^{-1})		experimental frequencies (cm^{-1})	
no.	B3LYP	B2PLYP	RR[b]	Raman[c]
ν_6	1623.0	1627.2	1617	1623
ν_7	1585.9	1593.0	1590	1593
ν_8	1538.8	1539.1	1538	1540
ν_9	1480.8	1482.9	1472	
ν_{10}	1453.4	1458.6		1459
ν_{11}	1382.2	1387.9	1382	1382
ν_{12}	1341.3	1347.4		
ν_{13}	1288.2	1292.9	1326	1327
ν_{14}	1252.7	1257.4	1250	1255
ν_{15}	1204.5	1210.4	1190	1192
ν_{16}	1163.4	1164.0		1159
ν_{17}	1136.9	1139.9	1134	1139
ν_{18}	1084.2	1084.1		1081
ν_{19}	1028.9	1031.5		1030
ν_{20}	867.7	863.9	870	871
ν_{21}	820.5	816.3	820	820
ν_{22}	670.0	667.5	669	668
ν_{23}	559.5	558.7	564	564
ν_{24}	543.7	540.6		547
ν_{25}	427.9	424.0	428	426
ν_{26}	372.2	371.2		
ν_{27}	283.8	284.1	290	286
MAD[d]	6.6	8.9		
MAX[d]	37.8 (ν_{13})	33.1 (ν_{13})		
MAD[e]	5.4	5.8		
MAX[e]	38.8 (ν_{13})	34.1 (ν_{13})		

[a] The calculated harmonic frequencies are scaled by a factor of 0.98. [b] Experimental RR frequencies in cyclohexane solution.[17] [c] Experimental Raman frequencies in CCl_4 solution.[38] [d] Mean absolute deviation (MAD) and maximal absolute deviation (MAX) with respect to the experimental RR frequencies. [e] MAD and MAX with respect to the experimental Raman frequencies.

The comparison between the theoretical and experimental RR spectra provides an assignment in global agreement with the one reported by Wang et al.[17] The only exception concerns the most intense RR band in the experimental spectrum at 1326 cm^{-1}, which is assigned here to the vibration ν_{13} at 1288.2 cm^{-1} instead of the vibration ν_{12} at 1341.3 cm^{-1}. This assignment is strongly motivated by the larger RR intensity calculated for ν_{13} in comparison to ν_{12} and is also in agreement with the assignment of the Raman spectrum. However, it should be noted that the frequency of ν_{13} shows the maximal absolute deviation (MAX) with respect to experimental results with an underestimation of about 38 cm^{-1}. This deviation of the ν_{13} frequency was already noted by Kovács et al.[38] and was possibly attributed to a Fermi resonance interaction. Such effects are not included in the present calculations, which employ the harmonic approximation. Moreover, the experimental IR frequencies in a CCl_4 solution[38] of the ν_{12} and ν_{13} vibrations are close, with values of 1333 and

Table 2. Vertical Excitation Energies (E^e) and Oscillator Strengths (f) of the First Singlet Excited State

	B3LYP geometry		B2PLYP geometry	
	E^e (eV)[a]	f	E^e (eV)[a]	f
BLYP	2.94 (−0.63)	0.0477	2.91 (−0.66)	0.0458
ωB97[b]	4.18 (0.61)	0.1749	4.18 (0.61)	0.1722
SCS-CC2[c]	4.08 (0.51)	0.1035	4.08 (0.51)	0.1016
ωB97X	4.07 (0.50)	0.1619	4.07 (0.50)	0.1588
M06-2X	4.00 (0.43)	0.1376	3.99 (0.42)	0.1342
CC2[c]	3.97 (0.40)	0.1065	3.97 (0.40)	0.1046
BMK	3.86 (0.29)	0.1188	3.85 (0.28)	0.1152
CAM-B3LYP	3.84 (0.27)	0.1302	3.82 (0.25)	0.1266
B3LYP	3.38 (−0.19)	0.0763	3.37 (−0.20)	0.0734
B3LYP-35	3.71 (0.14)	0.1032	3.69 (0.12)	0.0996
M06	3.45 (−0.12)	0.0848	3.43 (−0.14)	0.0816
HSE06	3.50 (−0.07)	0.0835	3.48 (−0.09)	0.0804
exptl.[d]	3.57	0.0689	3.57	0.0689

[a] The energy deviations with respect to experimental results are given in brackets. [b] Energies and oscillator strengths of the second singlet excited state. [c] Energies and oscillator strengths calculated in a vacuum. [d] Experimental energy and oscillator strength in a cyclohexane solution.[17]

1325 cm^{-1}, respectively. Therefore, it might be possible that the RR intensities of these two bands are superimposed in the experiment.

The vibrational frequencies of oNP were also calculated with the double-hybrid B2PLYP XC functional. It was shown recently[39] that this functional provides reliable vibrational frequencies and normal coordinates. From Table 1 it is seen that B2PLYP gives vibrational frequencies in close agreement with the B3LYP results. The larger deviation is found for the ν_7 vibration with a difference of about 7 cm^{-1}. It can also be mentioned that the normal coordinates obtained with both theoretical methods show similar nuclear displacements. Additionally, the mean absolute deviations (MAD) of the vibrational frequencies with respect to experimental results are rather small for both XC functionals, with MADs between 5.4 and 8.9 cm^{-1}. Such values are in agreement with previous works[29,39−42] and confirm the reliability of the B3LYP and B2PLYP functionals for the determination of ground state vibrational frequencies. Therefore, the geometries, frequencies, and normal coordinates obtained with these two force fields will be employed in the following to investigate the RR intensities of oNP.

3.2. Excited States. The vertical excitation energy and oscillator strength of the first allowed excited state of oNP were calculated with different XC functionals as well as with (SCS)-CC2 methods by employing the B3LYP and B2PLYP ground state geometries (Table 2). The experimental absorption spectrum in cyclohexane[17] shows a single unstructured band in the 400−300 nm range, which can be associated with the first singlet excited state of oNP. For each considered method, this state involves a transition from the HOMO to the LUMO orbitals (Figure 1), which present a transfer of electronic density going from the aromatic cycle and OH group to the NO_2 group. Therefore, a geometrical reorganization is expected to occur over the entire molecule after excitation to the excited state. This is also in agreement with the fact that several fundamental vibrations show RR activity in the 200−1700 cm^{-1} wavenumber range and are associated with normal coordinates distributed on the different parts of oNP.

From Table 2, it is seen that small differences are found between the excitation energies (<0.03 eV) and oscillator strengths calculated with B3LYP and B2PLYP. Of course, this is related to the similar geometries obtained with both methods, which present bond length differences lower than 0.004 Å. The comparison between the different XC functionals shows that the excitation energies and oscillator strengths are strongly dependent on the amount of HF exchange included in the functional. Indeed, the excitation energy calculated with the pure GGA functional BLYP is underestimated by 0.63 eV in comparison to experimental results (B3LYP geometry), whereas the hybrid functionals B3LYP, M06, and HSE06 including a moderate amount of HF exchange of 20, 27, and 25%, respectively, improve significantly the value of the excitation energy. Thus, the best agreement with respect to experimental results is found for the screened hybrid functional HSE06 with an underestimation of the excitation energy of only 0.07 eV (B3LYP geometry). Then, functionals with a larger amount of HF exchange show an overestimation of the excitation energy, as can be seen for B3LYP-35, BMK, and M06-2X, which incorporate 35, 42, and 54% of HF exchange, respectively. Of these functionals, B3LYP-35 provides the most accurate results with an overestimation of only 0.14 eV. Moreover, rather significant overestimations are obtained with the long-range corrected functionals CAM-B3LYP, ωB97, and ωB97X as well as with the (SCS)-CC2 methods, with CAM-B3LYP providing the best estimate. However, it should be mentioned that no solvent effects were included in the (SCS)-CC2 calculations. By approximating the solvatochromic shift with a B3LYP/IEFPCM calculation, the (SCS)-CC2 energies should be decreased by about 0.1 eV, which improves the CC2 excitation energy to a value very close to the BMK and CAM-B3LYP results. Moreover, it is seen in Table 2 that the oscillator strengths are overestimated in comparison to experimental results for all methods, except BLYP. Similarly to the excitation energies, the most accurate oscillator strengths are obtained with the XC functionals incorporating a moderate amount of HF exchange, i.e., B3LYP, HSE06, and M06, whereas the other methods provide oscillator strengths that are significantly overestimated. In the next step, how the accuracy on the excitation energies and oscillator strengths correlates to the accuracy on the RR spectra will be investigated.

3.3. Effect of the Computational Method on the *o*-Nitrophenol RR Spectrum. *3.3.1. RR Spectra Calculated with the B3LYP Force Field.* The STA RR spectra calculated with the B3LYP force field for the ground state and with different theoretical methods for the evaluation of the excited state gradients are presented in Figure 4 and are compared to the experimental spectrum. In order to provide a more quantitative comparison between the theoretical methods, the MAD and MAX of the relative RR intensities with respect to experimental results are reported in Table 3. First, it is seen that BLYP gives the larger MAD and shows a RR spectrum with too strong intensities in the 1300−1700 cm^{-1} wavenumber range and an incorrect intensity pattern for the ν_{14}, ν_{15}, and ν_{17} vibrations. Improvements are obtained for most of the intensities with the four hybrid functionals M06, B3LYP, HSE06, and B3LYP-35. However, the vibrations ν_6, ν_{11}, and ν_{22} still show noticeable overestimated intensities, whereas vibrations ν_8 and ν_{17} have a too weak RR intensity in comparison to experimental results. Despite

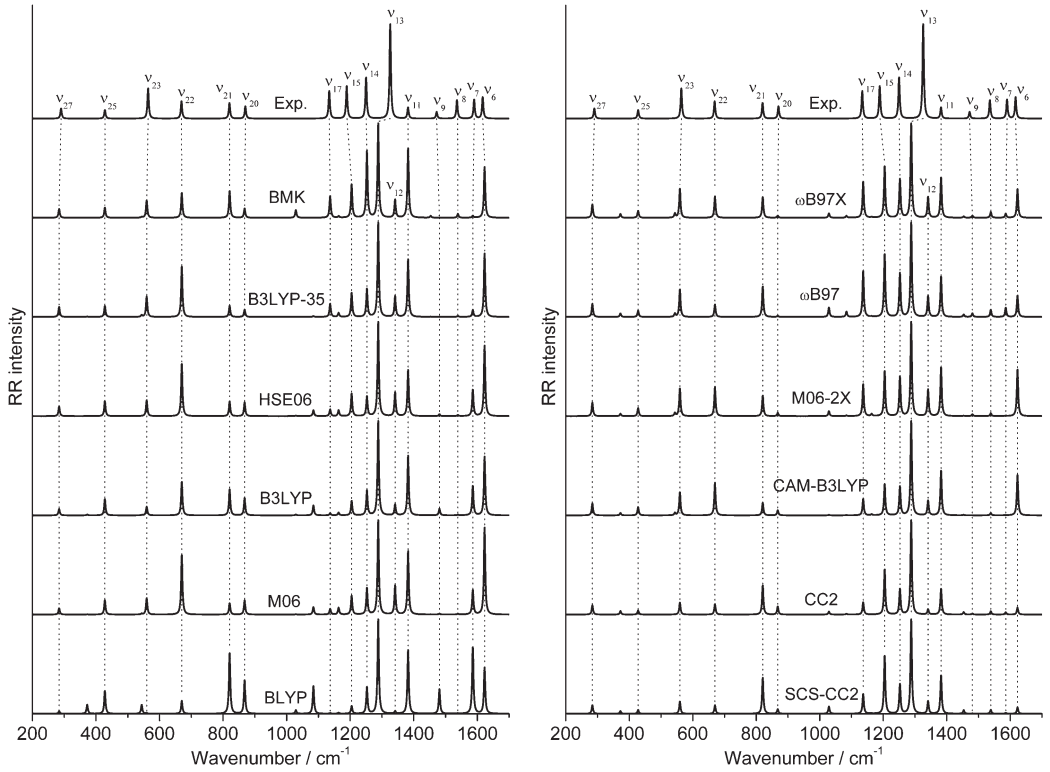

Figure 4. Comparison between the experimental RR spectrum[17] and the STA RR spectra calculated using the B3LYP force field in association with different methods for the evaluation of excited state gradients. The spectra are normalized with respect to vibration ν_{13}, and a Lorentzian function with a fwhm of 5 cm^{-1} is employed to broaden the transitions.

a large MAX value for vibration ν_{11}, the BMK functional provides a further improved MAD, mostly due to a better description of the ν_6, ν_{15}, ν_{17}, and ν_{22} RR intensities. Next, the RR spectra obtained with the (SCS)-CC2 methods present interesting differences with respect to the spectra calculated with DFT methods: (i) The vibrations ν_6, ν_7, and ν_8 are obtained with comparable intensities, which is in better agreement with experimental results even if their intensities are globally underestimated. (ii) Both ν_{11} and ν_{12} intensities are significantly reduced, which provides an additional confirmation for the assignment of vibrations ν_{11}, ν_{12}, and ν_{13}. (iii) CC2 gives the smallest value of MAX, with a deviation of only 0.193 for vibration ν_{23}, illustrating the overall good agreement obtained with this method. (iv) Similarly to the excitation energies, the use of SCS-CC2 does not provide an improvement in comparison to CC2. Moreover, smaller MADs are found with M06-2X and with the long-range corrected functionals CAM-B3LYP, ωB97, and ωB97X: (i) The ωB97X functional provides the smallest MAD with a value of only 0.094. (ii) The RR intensities of the low-frequency modes in the 200−900 cm^{-1} wavenumber range are better reproduced with these functionals, even if the intensity of ν_{20} is underestimated with the ωB97(X) methods. (iii) The intensities of ν_{14}, ν_{15}, and ν_{17} are in overall good agreement with experimental results, despite an overestimation in the case of ωB97. (iv) the overestimation of the ν_{11} intensity is reduced in comparison to other functionals but is still larger than the one obtained with CC2. (v) The ωB97(X) functionals provide an improved description of the intensities in the 1400−1700 cm^{-1} wavenumber range in comparison to the CAM-B3LYP, M06-2X, and (SCS)-CC2 methods. Finally, the comparison between the calculations and experimental results shows that the accuracy of the simulated RR spectra (Table 3) is not correlated with the accuracy of the excitation energies and oscillator strengths (Table 2). This is clearly seen for the functionals ωB97(X), which provide the RR spectra with the lowest MADs but give the

Table 3. Mean Absolute Deviations (MAD) and Maximal Absolute Deviations (MAX) of the Relative RR Intensities with Respect to Experimental Results[a]

	B3LYP force field		B2PLYP force field	
	MAD[b]	MAX	MAD	MAX
BLYP	0.264 (0.275)	0.559 (ν_{11})	0.257	0.631 (ν_{11})
M06	0.203 (0.222)	0.697 (ν_6)	0.231	0.875 (ν_{11})
B3LYP	0.180 (0.195)	0.516 (ν_{11})	0.192	0.686 (ν_{11})
HSE06	0.170 (0.189)	0.523 (ν_6)	0.192	0.623 (ν_{11})
B3LYP-35	0.162 (0.172)	0.493 (ν_{11})	0.187	0.727 (ν_{11})
BMK	0.148 (0.148)	0.622 (ν_{11})	0.190	0.782 (ν_{11})
SCS-CC2[c]	0.141 (0.144)	0.290 (ν_{11})	0.133	0.404 (ν_{11})
CC2[c]	0.120 (0.122)	0.193 (ν_{23})	0.118	0.216 (ν_{11})
CAM-B3LYP	0.116 (0.126)	0.356 (ν_{11})	0.133	0.511 (ν_{11})
M06-2X	0.115 (0.118)	0.400 (ν_{11})	0.134	0.621 (ν_{11})
ωB97	0.109 (0.108)	0.322 (ν_{15})	0.110	0.451 (ν_{11})
ωB97X	0.094 (0.097)	0.309 (ν_{11})	0.094	0.462 (ν_{11})

[a] The experimental RR spectrum in cyclohexane solution at 355 nm is from ref 17. The comparison is made by normalizing to unity the intensity of vibration ν_{13} in both calculated and experimental RR spectra. [b] The MADs with respect to the experimental RR spectrum at 369 nm are given in brackets. [c] Excited state derivatives calculated in a vacuum.

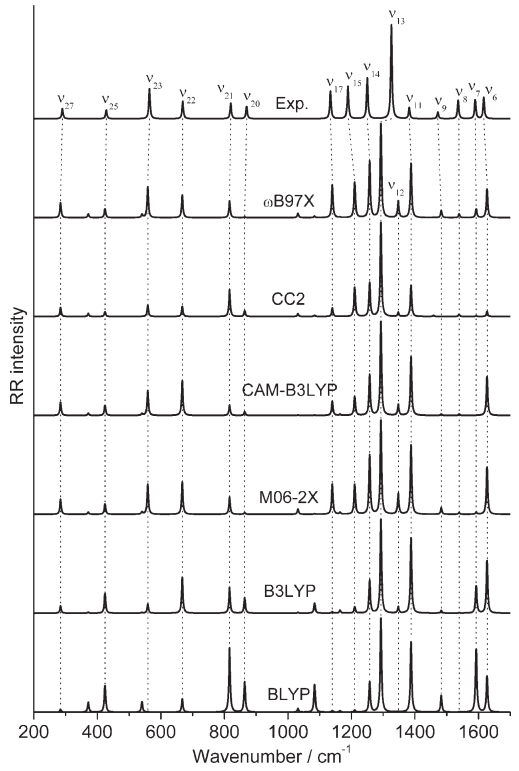

Figure 5. Comparison between the experimental RR spectrum[17] and the STA RR spectra calculated using the B2PLYP force field in association with different methods for the evaluation of excited state gradients. The spectra are normalized with respect to vibration ν_{13}, and a Lorentzian function with a fwhm of 5 cm^{-1} is employed to broaden the transitions.

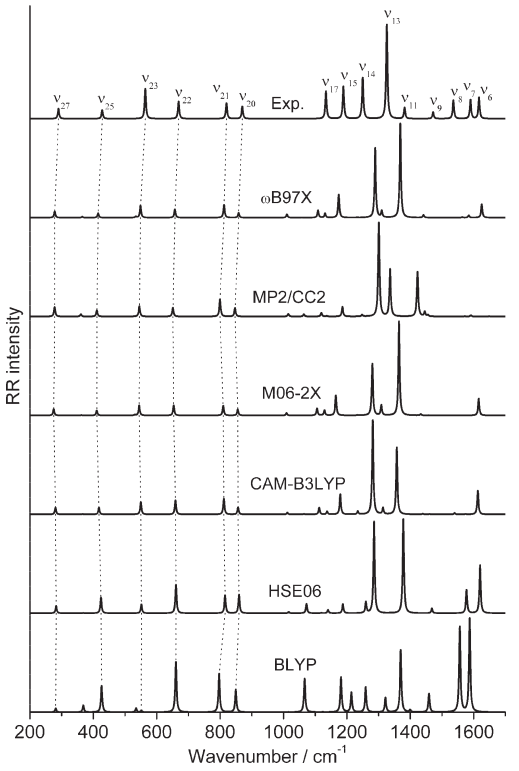

Figure 6. Comparison between the experimental RR spectrum[17] and the STA RR spectra calculated using different computational methods. The spectra are normalized with respect to vibration ν_{13}, and a Lorentzian function with a fwhm of 5 cm^{-1} is employed to broaden the transitions.

largest overestimations of both the excitation energy and the oscillator strength.

Additionally, in order to confirm the validity of the STA, the RR spectrum was simulated using the ωB97X functional by including the vibronic structure of the excited state according to a method described elsewhere.[31] This allows the dependency of the RR spectrum with respect to the excitation wavelength to be accounted for. Thus, the simulation of the RR spectrum for an excitation wavelength of 355 nm provides a MAD of 0.102 and a MAX of 0.297 (for vibration ν_{11}). These values are very close to those obtained within the STA and consequently justify the use of this approximation for the purpose of assessing the accuracy of different theoretical methods. This is also corroborated by the small dependency of the experimental RR intensities with respect to the excitation wavelength.[17] Indeed, the MADs obtained by comparing the simulated intensities with the experimental spectrum recorded for an excitation wavelength of 369 nm (Table 3) show the same trends as those obtained by comparing to the 355 nm experimental spectrum.

3.3.2. RR Spectra Calculated with the B2PLYP and Other Force Fields. The RR spectra obtained with the B2PLYP force field (Figure 5) present no significant improvements in comparison to those obtained with the B3LYP force field (Figure 4). Indeed, as can be seen from Table 3, most of the MADs are larger or very close to the one calculated with the B3LYP force field. The only small improvements are found for the MADs of the (SCS)-CC2 methods, which are closer to those obtained with the XC functionals CAM-B3LYP, M06-2X, and ωB97(X). Additionally, all of the MAX values corresponding to vibration ν_{11} are increased in comparison to B3LYP, indicating that this mode is less accurately described with the B2PLYP force field. Therefore, on the basis of the vibrational frequencies (Table 1) and of the RR intensities (Table 3), it appears that B2PLYP does not improve the ground state properties of oNP in comparison to B3LYP.

Furthermore, it is interesting to investigate the accuracy of the RR spectra in the situation where the same theoretical method is employed for both the ground and the excited state calculations. Thus, Figure 6 shows the RR spectra obtained with the DFT methods BLYP, HSE06, CAM-B3LYP, M06-2X, and ωB97X as well as the spectrum obtained using MP2 for the ground state properties and CC2 for the excited state gradients. It should be mentioned that comparable normal coordinates are found with all methods for the ν_{20}, ν_{21}, ν_{22}, ν_{23}, ν_{25}, and ν_{27} vibrations, which leads to a straightforward assignment of these vibrations. However, the normal coordinates of all of the vibrations in the 1000−1700 cm^{-1} wavenumber range are found to be strongly different between the theoretical methods. As can be seen from Figure 6, this leads to important differences in the simulated RR intensities in this wavenumber window. It appears also clearly that no spectrum improves over those calculated with the B3LYP or B2PLYP force fields, but instead large discrepancies with respect to experimental results are obtained. This also shows that an assignment of the vibrational bands in the 1000−1700 cm^{-1} wavenumber range is hardly possible by employing these methods for the ground state properties of oNP and consequently that the geometries and normal coordinates obtained with these force fields are less accurate than those calculated with B3LYP and

B2PLYP. This result is also in agreement with a recent work[39] which showed that HSE06, CAM-B3LYP, M06-2X, and ωB97X provide less accurate vibrational frequencies than B3LYP or B2PLYP.

4. CONCLUSIONS

The RR relative intensities of *o*-nitrophenol were investigated theoretically with the aim of assessing the accuracy of excited state calculations based on DFT and CC2 approaches. The comparison between simulated Raman and RR spectra with experimental results allowed a reliable assignment of the vibrational bands. Thus, it is found that B3LYP provides the best estimate of the ground state properties, while B2PLYP calculations show no improvement and even a slightly reduced accuracy in comparison to B3LYP. Moreover, the results obtained with the BLYP, HSE06, CAM-B3LYP, M06-2X, ωB97X, and MP2 methods present significantly less accurate vibrational frequencies and normal coordinates, leading to important differences in their respective RR spectrum, which show large discrepancies with respect to experimental results. However, the use of the B3LYP force field for the ground state in association with different methods for the excited state gradients shows a noticeable improvement of the accuracy of RR intensities. Thus, XC functionals including a large amount of HF exchange and long-range corrections like M06-2X, CAM-B3LYP, and ωB97(X) provide the most accurate RR spectra. The RR intensities obtained with the best XC functionals are of comparable accuracy to those obtained with CC2 calculations, which shows that these approaches should be considered more often in the future for simulating RR intensities of middle-sized to large systems. It is also seen that the accuracy of the excited state gradients does not correlate with the accuracy of the excitation energies and oscillator strengths, for which XC functionals with lesser HF exchange like B3LYP, M06, and HSE06 provide more accurate results in the case of oNP. This result also indicates that in addition to evaluating vertical excitation energies, the assessment of excited state gradients offers the possibility of having a complementary view about the performance of newly developed functionals in predicting excited state properties. Finally, the study demonstrates that an accurate description of both ground and excited state properties remains a challenging task, even for recently developed theoretical approaches. However, a significant improvement of the RR relative intensities can be obtained using a hybrid approach, in which the ground and excited states are described by two separate theoretical methods.

AUTHOR INFORMATION

Corresponding Author

*E-mail: julien.guthmuller@uni-jena.de.

ACKNOWLEDGMENT

The author thanks the Carl-Zeiss Stiftung for financial support and the Thüringer Ministerium für Bildung, Wissenschaft und Kultur (PhotoMIC). All of the calculations have been performed at the Universitätsrechenzentrum of the Friedrich-Schiller University of Jena and on the HP computers of the Theoretical Chemistry group. The author also thanks Prof. Leticia González for helpful discussions as well as Martin Elstner and Marcus Schulze for performing preliminary calculations on oNP.

REFERENCES

(1) Silva-Junior, M. R.; Schreiber, M.; Sauer, S. P. A.; Thiel, W. *J. Chem. Phys.* **2008**, *129*, 104103.
(2) Jacquemin, D.; Wathelet, V.; Perpète, E. A.; Adamo, C. *J. Chem. Theory Comput.* **2009**, *5*, 2420–2435.
(3) Jacquemin, D.; Perpète, E. A.; Ciofini, I.; Adamo, C. *J. Chem. Theory Comput.* **2010**, *6*, 1532–1537.
(4) Goerigk, L.; Grimme, S. *J. Chem. Phys.* **2010**, *132*, 184103.
(5) Hellweg, A.; Grün, S. A.; Hättig, C. *Phys. Chem. Chem. Phys.* **2008**, *10*, 4119.
(6) Silva-Junior, M. R.; Schreiber, M.; Sauer, S. P. A.; Thiel, W. *J. Chem. Phys.* **2010**, *133*, 174318.
(7) Schreiber, M.; Silva-Junior, M. R.; Sauer, S. P. A.; Thiel, W. *J. Chem. Phys.* **2008**, *128*, 134110.
(8) Miura, M.; Aoki, Y.; Champagne, B. *J. Chem. Phys.* **2007**, *127*, 084103.
(9) Guthmuller, J.; Zutterman, F.; Champagne, B. *J. Chem. Theory Comput.* **2008**, *4*, 2094–2100.
(10) Guillaume, M.; Liégeois, V.; Champagne, B.; Zutterman, F. *Chem. Phys. Lett.* **2007**, *446*, 165–169.
(11) Santoro, F.; Improta, R.; Lami, A.; Bloino, J.; Barone, V. *J. Chem. Phys.* **2007**, *126*, 084509.
(12) Dierksen, M.; Grimme, S. *J. Phys. Chem. A* **2004**, *108*, 10225–10237.
(13) Albrecht, A. C. *J. Chem. Phys.* **1961**, *34*, 1476.
(14) Myers, A. B. *Chem. Rev.* **1996**, *96*, 911–926.
(15) Long, D. A. *The Raman Effect: A Unified Treatment of the Theory of Raman Scattering by Molecules*; John Wiley & Sons Ltd: New York, 2002.
(16) Heller, E. J.; Sundberg, R.; Tannor, D. *J. Phys. Chem.* **1982**, *86*, 1822–1833.
(17) Wang, Y.; Wang, H.; Zhang, S.; Pei, K.; Zheng, X.; Lee Phillips, D. *J. Chem. Phys.* **2006**, *125*, 214506.
(18) Christiansen, O.; Koch, H.; Jørgensen, P. *Chem. Phys. Lett.* **1995**, *243*, 409–418.
(19) Frisch, M. J.; Trucks, G. W.; Schlegel, H. B.; Scuseria, G. E.; Robb, M. A.; Cheeseman, J. R.; Scalmani, G.; Barone, V.; Mennucci, B.; Petersson, G. A.; Nakatsuji, H.; Caricato, M.; Li, X.; Hratchian, H. P.; Izmaylov, A. F.; Bloino, J.; Zheng, G.; Sonnenberg, J. L.; Hada, M.; Ehara, M.; Toyota, K.; Fukuda, R.; Hasegawa, J.; Ishida, M.; Nakajima, T.; Honda, Y.; Kitao, O.; Nakai, H.; Vreven, T.; Montgomery, Jr., J. A.; Peralta, J. E.; Ogliaro, F.; Bearpark, M.; Heyd, J. J.; Brothers, E.; Kudin, K. N.; Staroverov, V. N.; Kobayashi, R.; Normand, J.; Raghavachari, K.; Rendell, A.; Burant, J. C.; Iyengar, S. S.; Tomasi, J.; Cossi, M.; Rega, N.; Millam, J. M.; Klene, M.; Knox, J. E.; Cross, J. B.; Bakken, V.; Adamo, C.; Jaramillo, J.; Gomperts, R.; Stratmann, R. E.; Yazyev, O.; Austin, A. J.; Cammi, R.; Pomelli, C.; Ochterski, J. W.; Martin, R. L.; Morokuma, K.; Zakrzewski, V. G.; Voth, G. A.; Salvador, P.; Dannenberg, J. J.; Dapprich, S.; Daniels, A. D.; Farkas, Ö.; Foresman, J. B.; Ortiz, J. V.; Cioslowski, J.; Fox, D. J. *Gaussian 09*, Revision A.02; Gaussian Inc.: Wallingford, CT, 2009.
(20) Head-Gordon, M.; Head-Gordon, T. *Chem. Phys. Lett.* **1994**, *220*, 122–128.
(21) Becke, A. D. *Phys. Rev. A* **1988**, *38*, 3098.
(22) Lee, C.; Yang, W.; Parr, R. G. *Phys. Rev. B* **1988**, *37*, 785.
(23) Becke, A. D. *J. Chem. Phys.* **1993**, *98*, 5648.
(24) Henderson, T. M.; Izmaylov, A. F.; Scalmani, G.; Scuseria, G. E. *J. Chem. Phys.* **2009**, *131*, 044108.
(25) Yanai, T.; Tew, D. P.; Handy, N. C. *Chem. Phys. Lett.* **2004**, *393*, 51–57.
(26) Zhao, Y.; Truhlar, D. G. *Theor. Chem. Acc.* **2007**, *120*, 215–241.
(27) Chai, J.; Head-Gordon, M. *J. Chem. Phys.* **2008**, *128*, 084106.
(28) Grimme, S. *J. Chem. Phys.* **2006**, *124*, 034108.
(29) Merrick, J. P.; Moran, D.; Radom, L. *J. Phys. Chem. A* **2007**, *111*, 11683–11700.
(30) Tomasi, J.; Mennucci, B.; Cammi, R. *Chem. Rev.* **2005**, *105*, 2999–3094.

(31) Guthmuller, J.; Champagne, B. *J. Chem. Phys.* **2007**, *127*, 164507.
(32) Boese, A. D.; Martin, J. M. L. *J. Chem. Phys.* **2004**, *121*, 3405.
(33) Hättig, C.; Weigend, F. *J. Chem. Phys.* **2000**, *113*, 5154.
(34) Köhn, A.; Hättig, C. *J. Chem. Phys.* **2003**, *119*, 5021.
(35) *TURBOMOLE V6.2*; University of Karlsruhe and Forschungszentrum Karlsruhe GmbH: Karlsruhe, Germany, 2010. Available from http://www.turbomole.com (accessed March 2011).
(36) Weigend, F.; Ahlrichs, R. *Phys. Chem. Chem. Phys.* **2005**, *7*, 3297.
(37) Wilson, E. B., Jr.; Decius, J. C.; Cross, P. C. *Molecular Vibrations*; McGraw-Hill: New York, 1955.
(38) Kovács, A.; Izvekov, V.; Keresztury, G.; Pongor, G. *Chem. Phys.* **1998**, *238*, 231–243.
(39) Biczysko, M.; Panek, P.; Scalmani, G.; Bloino, J.; Barone, V. *J. Chem. Theory Comput.* **2010**, *6*, 2115–2125.
(40) Jiménez-Hoyos, C. A.; Janesko, B. G.; Scuseria, G. E. *Phys. Chem. Chem. Phys.* **2008**, *10*, 6621.
(41) Guthmuller, J.; González, L. *Phys. Chem. Chem. Phys.* **2010**, *12*, 14812.
(42) Guthmuller, J.; Cecchet, F.; Lis, D.; Caudano, Y.; Mani, A. A.; Thiry, P. A.; Peremans, A.; Champagne, B. *ChemPhysChem* **2009**, *10*, 2132–2142.